JOURNAL OF SPACECRAFT AND ROCKETS
Vol. 43, No. 5, September–October 2006

Mars Exploration Rover Six-Degree-of-Freedom Entry Trajectory Analysis

Prasun N. Desai,* Mark Schoenenberger,† and F. M. Cheatwood‡
NASA Langley Research Center, Hampton, Virginia 23681

DOI: 10.2514/1.6008

The Mars Exploration Rover mission delivered the rovers Spirit and Opportunity to the surface of Mars using the same entry, descent, and landing scenario that was developed and successfully implemented by Mars Pathfinder. This investigation describes the premission trajectory analysis that was performed for the hypersonic portion of the Mars Exploration Rover entry up to parachute deployment. In this analysis, a six-degree-of-freedom trajectory simulation of the entry is performed to determine the entry characteristics of the capsules. In addition, a Monte Carlo dispersion analysis is also performed to statistically assess the robustness of the entry design to off-nominal conditions to ensure that all entry requirements are satisfied. The premission results show that the attitude at peak heating and parachute deployment are well within entry limits. In addition, the parachute deployment dynamic pressure and Mach number are also well within the design requirements.

Nomenclature

C_A	=	axial force coefficient
C_D	=	drag force coefficient
C_m	=	static pitching moment coefficient
C_{mq}	=	dynamic pitch damping coefficient
$C_{m\alpha}$	=	static stability parameter
C_N	=	normal force coefficient
C_n	=	static yawing moment coefficient
C_{nr}	=	dynamic yaw damping coefficient
C_Y	=	side force coefficient
I_{xx}, I_{yy}, I_{zz}	=	moments of inertia, kg–m^2
I_{xy}, I_{xz}, I_{yz}	=	cross products of inertia, kg–m^2
Kn	=	Knudsen number
L/D	=	lift-to-drag ratio
M	=	Mach number
x_{cg}	=	axial center-of-gravity location (from capsule nose), m
α	=	angle of attack, deg
α_T	=	total angle of attack, deg

I. Introduction

THE Mars Exploration Rover (MER) mission's Spirit and Opportunity spacecrafts were successfully launched on 10 June 2003 and 7 July 2003, respectively. The Landers were targeted to the equatorial region of Mars with Spirit landing in Gusev crater (14.59 deg S, 175.3 deg E) on 04 January 2004 and Opportunity landing in Meridiani Plains (1.98 deg S, 5.94 deg W) on 25 January 2004. Each Lander carried a rover designed to explore the surface of Mars making in situ measurements. However, unlike the Mars Pathfinder Sojourner rover, these rovers are larger and more capable of accommodating an increased suite of science instruments, and are able to traverse greater distances during surface operations. Roncoli and Ludwinski [1] gives an overview of the MER mission.

Both Landers delivered the rovers to the surface utilizing the same entry, descent, and landing (EDL) scenario that was developed and successfully implemented by Mars Pathfinder (MPF) [2]. The capsule decelerated with the aid of an aeroshell, a supersonic parachute, retrorockets, and air bags for safely landing on the surface (see Fig. 1). Steltzner et al. [3] gives a description of the EDL system.

In addition, the MER Landers utilized the same capsule configuration (a 70 deg sphere cone) as MPF as shown in Fig. 2. However, the entry similarities between MPF and MER end there. The MER design entry mass is much higher, the entry velocity is lower, and the entry local time is different. These differences lead to a different entry profile for MER as it descends through Mars's atmosphere. Figure 3 compares the entry profiles for MER, MPF, and Viking. As seen, the MER entry is bounded by the Viking and MPF profiles. Table 1 summarizes the entry characteristics of Viking, MPF, and MER.

Approximately 15 min prior to entry, the capsule was separated from the cruise stage. The capsule has no active guidance or control system, so that the 2 rpm spin rate maintains its entry attitude during coast until atmospheric interface (nominally 0 deg angle of attack). Throughout the atmospheric entry, the passive capsule relies solely on aerodynamic stability for performing a controlled descent through all aerodynamic flight regimes: free molecular, transitional, hypersonic-continuum, and supersonic. The capsule must possess sufficient aerodynamic stability to minimize any angle-of-attack excursions during the severe heating environment. Additionally, this stability must persist through the supersonic regime to maintain a controlled attitude at parachute deployment.

This paper describes the premission trajectory analysis that was performed for the hypersonic portion of the MER entry up to parachute deployment. In this analysis, a 6 degree-of-freedom (DOF) trajectory simulation of the entry (from cruise-stage separation to parachute deployment) is performed to determine the entry characteristics of the MER capsules. Of specific interest is the attitude dynamics of the capsule during the descent near peak heating and at parachute deployment, along with the parachute deployment conditions (dynamics pressure and Mach number). This information is necessary for defining requirements for the thermal protection and parachute subsystems. In addition, a Monte Carlo analysis is also performed to statistically assess the robustness of the entry design to off-nominal conditions to assure that all EDL requirements are satisfied.

Presented at the AAS/AIAA Astrodynamics Specialists Conference, Big Sky, Montana, 3–7 August 2003; received 24 October 2003; revision received 2 January 2006; accepted for publication 2 January 2006.

*Senior Aerospace Engineer, Exploration Systems Engineering Branch, Systems Engineering Directorate; prasun.n.desai@nasa.gov. Associate Fellow AIAA.

†Aerospace Engineer, Exploration Systems Engineering Branch, Systems Engineering Directorate; m.schoenenberger-1@nasa.gov.

‡Senior Aerospace Engineer, Space Operations & Space Technology Programs, Exploration Systems & Space Operations Technology Directorate; f.m.cheatwood@nasa.gov.

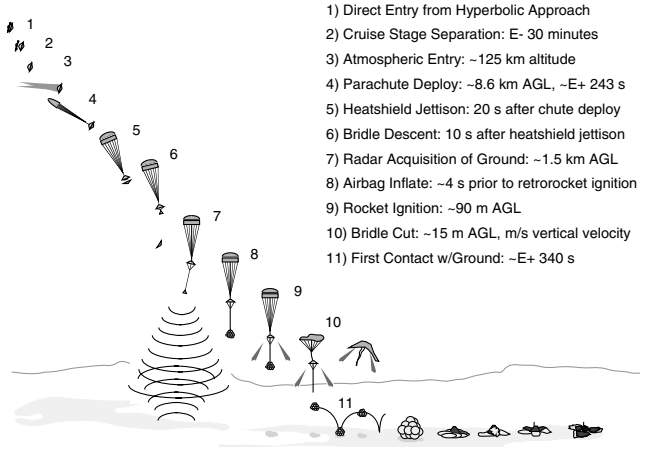

Fig. 1 MER entry, descent, and landing sequence.

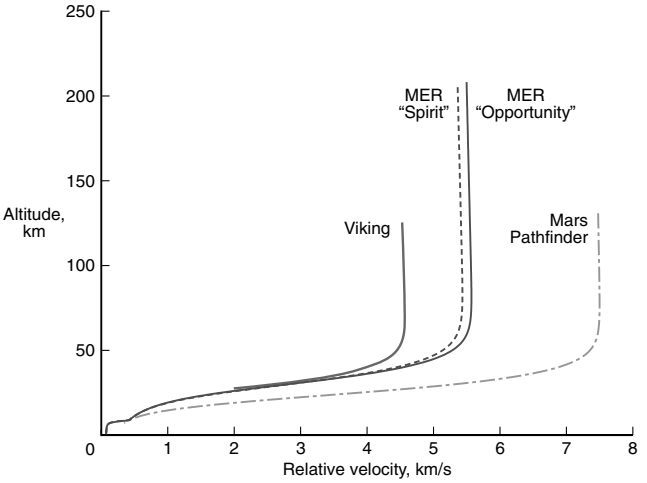

Fig. 3 Entry profile comparison.

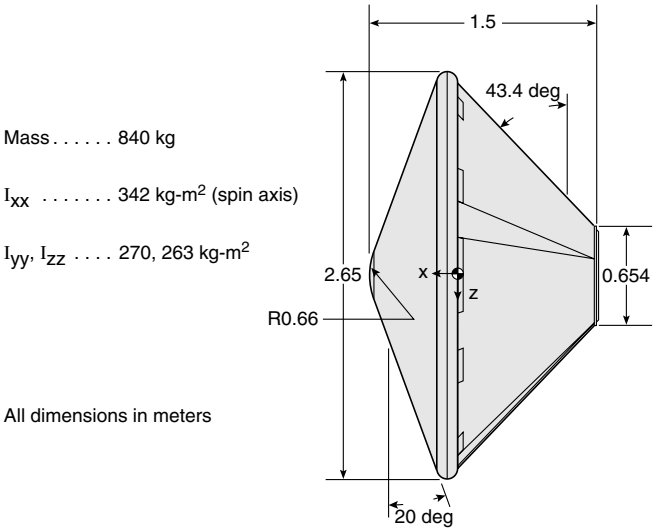

Fig. 2 MER entry capsule configuration.

II. Analysis

A. Aerodynamics

The aerodynamic database utilized for the MER capsule in the trajectory simulation analyses is constructed from a variety of computational and experimental sources, each chosen as the most appropriate method for the flight regime for which they are employed. The general structure of the database is a matrix of pitch damping, pitching moment, and normal and axial force coefficients defined for a range of angles of attack and speeds. An overlapping parabola interpolation scheme is employed to smoothly blend the aerodynamics between the data points and different flight regimes. For a given flight condition and capsule attitude, the database provides estimates of C_A, C_N, C_Y, C_m, C_n, C_{mq}, and C_{nr} for use in six-DOF simulations. This approach is essentially the same as that utilized for MPF [4]. However, the flow conditions for each data point are tailored to the MER entry trajectory, and a significant number of additional data points have been incorporated to increase the fidelity of this database. In addition, experimental work was performed to characterize the pitch damping of the MER capsule at supersonic conditions, and a large number of additional supersonic computational fluid dynamic (CFD) solutions were performed to increase confidence in the predictions of the capsule attitude at parachute deployment.

The variety of sources for the aerodynamics is required because the MER capsule traverses many different flow regimes (free molecular, transitional, hypersonic-continuum, supersonic) during its entry. The different flight regimes are defined by the dominant flow physics of the particular portion of the entry trajectory. The regimes, starting from atmospheric interface, include the following: free molecular, in which the particles of the atmosphere are modeled individually without interaction with each other; transitional, in which collisions among atmosphere molecules are important, but the flow cannot be modeled as a continuum; hypersonic-continuum, in which the flow is governed by the Navier–Stokes equations (with possible nonequilibrium gas chemistry effects), and negligible base pressure contributions to the aerodynamics; and supersonic, in which flow chemistry is in equilibrium and base pressure becomes an important part of the vehicle aerodynamics. A schematic of the database and these regimes is shown in Fig. 4.

The free molecular aerodynamic calculations were performed with the DACFREE code [5]. In the transitional flow regime, direct simulation Monte Carlo (DSMC) calculations were performed using the DAC code [6]. In the hypersonic and supersonic continuum regimes, a matrix of solutions from the computational fluid dynamics code LAURA (Langley Aerothermodynamic Upwind Relaxation

Table 1 Comparison of entry characteristics

	Viking I, II	Mars Pathfinder	MER A, B
Forebody geometry, deg	70	70	70
Aftbody geometry, deg	39/62 (biconic)	49	49
Relative entry velocity, km/s	4.5, 4.42	7.6	5.4, 5.55
Relative entry FPA, deg	−17.6	−13.8	−12
Entry local time	——	Predawn	Afternoon
Mass, kg	930	585	840
$m/(C_D A)$, kg/m^2	63.7	62.3	89.8
x_{cg}/D	0.221	0.27	0.27
Nominal α, deg	−11.1	0	0
L/D	0.18	0	0
Guidance & control	3-axis (active)	Spin stabilized	Spin stabilized

Algorithm) [7] describe the aerodynamics. These sources are blended to form a comprehensive database, which describe the aerodynamics of the MER capsule for the expected flight conditions.

Although LAURA solutions over the entire capsule were calculated for Mach numbers below 6, only the forebody contributions were included in the aerodynamic coefficients. In this regime, resolving the backshell pressure distribution of the flow field accurately for blunt bodies is very difficult. Therefore, a base pressure correction was applied to the axial force coefficient to account for the contribution from the capsule backshell. This correction was developed from Viking flight data [8] and was used in the same fashion for MPF. No correction was added to the pitching moment or normal force coefficients, because the effect on these coefficients is minimal. The success of both the Viking and MPF missions validate this approach. Figure 5 shows the matrix of LAURA solutions in the MER database.

Figure 6 shows a surface plot of $C_{m\alpha}$ in the continuum regime. At two velocities in the hypersonic regime, the pitching moment coefficient becomes positive at low angles of attack (<2 deg), indicating that the capsule is statically unstable in these regions. These instabilities are bounded, because as the angle of attack increases above 2 deg, the pitching moment becomes negative leading to a stable behavior. The bounded instability at 5.5 km/s (Mach 27) is due to the gas chemistry of the forebody flow changing from nonequilibrium to equilibrium. The bounded instability at 3.6 km/s (Mach 16) occurs because of a movement of the sonic line on the leeward side of the capsule from the shoulder to the spherical nose cap. These instabilities were predicted for MPF with LAURA and their existence and location was verified with flight data [9]. These instabilities predicted for MER are less severe than MPF. This consequence is primarily due to the lower entry velocity that results in less energetic chemical reactions.

The pitch damping characteristics of the MER capsule were determined experimentally through an extensive series of ballistic range tests. Presently, computational methods cannot predict damping behavior well. These tests were conducted at the Aeroballistic Research Facility at Eglin Air Force Base, where 70-mm-diam models were shot from a powder-charge gun at supersonic speeds down a 200 m range. The range is instrumented with 50 spark shadowgraph stations. Shadowgraphs taken from two orthogonal views at each station provided the model position and time as it flew past. The model trips a light beam at each station that simultaneously initiates the spark light source for the shadowgraphs and marks the time of the exposure. A total of 26 shots were performed having a range of initial attitudes and Mach numbers, along with three model center-of-gravity positions ($x_{cg}/D = 0.27$, 0.30 and 0.33), because the final location was not well known during the design phase. With this data of time, position, and attitude, data reduction efforts were conducted to extract the pitch damping coefficient curves using parameter identification methods [10].

Figure 7 shows the pitch damping coefficient C_{mq} versus Mach number and angle of attack. Note the low-speed, low-angle region where C_{mq} is positive, indicating that the MER capsule is dynamically unstable (i.e., excitation rather than damping). As a result, the capsule attitude increases while in this region. Negative C_{mq} values indicate that the capsule is dynamically stable (i.e., the attitude will damp out). This behavior is in qualitative agreement with Viking forced oscillation data [11]. This dynamic instability is bounded similar to the hypersonic static instabilities. As the capsule angle of attack increases, C_{mq} becomes negative damping out the attitude. This behavior tends toward a limit cycle phenomenon.

The supersonic pitch damping coefficient is a function of capsule geometry and center-of-gravity location. As a result, the Viking forced oscillation data is not appropriate for other configurations (see Table 1); although, this data was used in the MPF database because no ballistic range tests were performed for that mission. Consequently, the MPF capsule attitude was underpredicted in this supersonic flight region [2]. This ballistic range data reveal that the MER

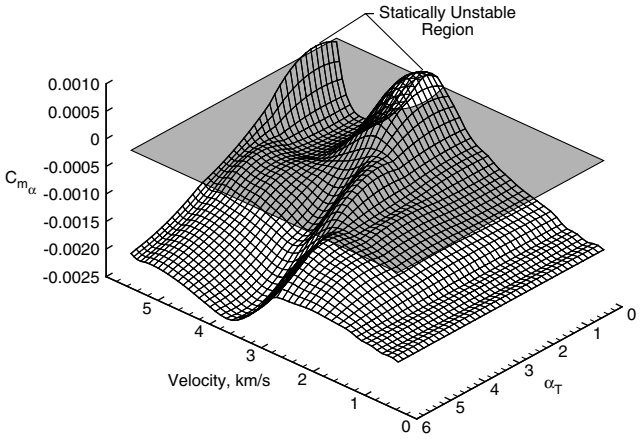

Fig. 6 LAURA hypersonic/supersonic $C_{m\alpha}$ (per degree) surface.

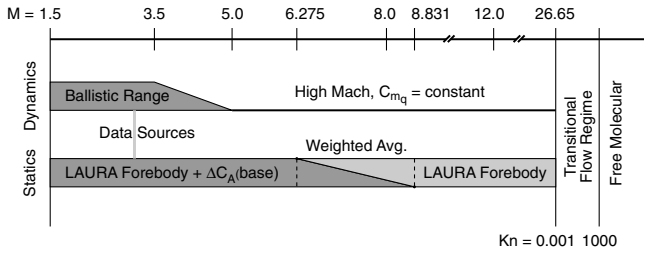

Fig. 4 Schematic of MER aerodynamic database.

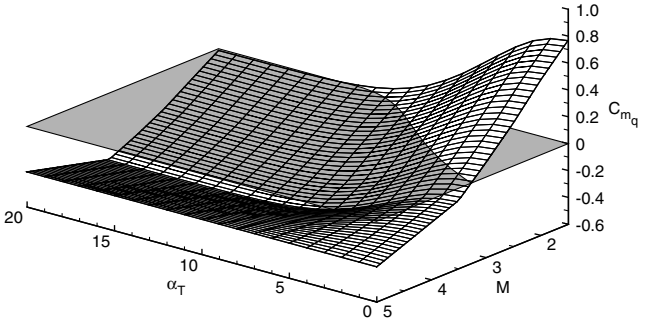

Fig. 7 Supersonic pitch damping surface from ballistic range data.

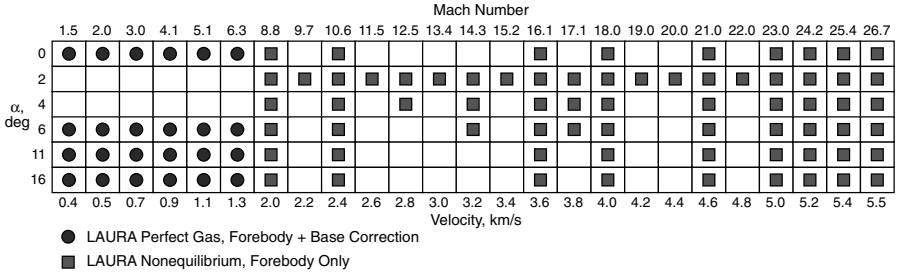

Fig. 5 Matrix of LAURA CFD solutions used in MER aerodynamic database.

Table 2 Exoatmospheric mission uncertainties

	3–σ Variance
Mass properties	
Center of gravity offset along axis of symmetry	±20 mm
Center of gravity offset off spin axis	±2.8 mm
Moments of inertia (I_{xx}, I_{yy}, I_{zz})	±10%, ±10%, ±10%
Cross product of inertia (I_{xy}, I_{xz}, I_{yz})	±1.6 kg–m^2, ±2.0 kg–m^2, ±1.6 kg–m^2
Postseparation state	
State vector (flight-path angle variation)	±0.13 deg
Pitch and yaw attitude	±1.7 deg, ±2.69 deg
Pitch and yaw rates	±0.4 deg/s, ±0.4 deg/s
Roll rate	±1.2 deg/s

Table 3 Atmospheric mission uncertainties

	3–σ Variance
Aerodynamic	
Free molecular aerodynamics	
C_A	±5%
C_N, C_Y	±0.01
C_m, C_n	±0.005
Hypersonic-continuum aerodynamics	
C_A	±5%
C_N, C_Y	±0.01
C_m, C_n	±0.003
Supersonic continuum aerodynamics	
C_A	±10%
C_N, C_Y	±0.01
C_m, C_n	±0.005
Free molecular dynamic stability coefficients, C_{mq}, C_{nr}	±0.09
Hypersonic dynamic stability coefficients, C_{mq}, C_{nr}	±0.09
Supersonic dynamic stability coefficients, C_{mq}, C_{nr}	[+100%, −50%] + [0 to 0.1][a]
Density above 60 km	±45%
Density below 60 km	±15%
Winds above 60 km	±80 m/s
Winds below 60 km	±40 m/s

[a]Uncertainty sampled using a uniform distribution.

(and MPF) capsule configuration is more dynamically unstable than the Viking configuration. As a result, the MER capsule oscillations will grow to larger amplitudes than if the Viking data had been utilized. Schoenenberger et al. [10,12] describe the MER aerodynamics database in detail.

B. Trajectory Simulation

The trajectory analysis is performed using the six-DOF version of the program to optimize simulated trajectories (POST) [13]. This program has been utilized previously for similar applications [4,14,15]. The trajectory simulation begins post-cruise-stage separation of the MER capsule, continues through atmospheric entry, and ends at parachute deployment. The trajectory analysis incorporates atmospheric and gravitational models, cruise-stage/capsule separation attitude and attitude rates, mass properties, and the previously described aerodynamics. The validity of the present approach has been demonstrated through comparisons between the MPF preflight predictions of the flight dynamics and the actual flight data, which show a very good agreement [2,9]. The Kass–Schofield atmosphere model utilized for the entry was specifically developed for the MER mission. This model takes into account the specific MER season, local time, and landing location in estimating the nominal and dispersed density and wind profiles.

During the entry, off-nominal conditions may arise that affect the descent profile. These off-nominal conditions can originate from numerous sources, such as capsule mass property measurement uncertainties, cruise-stage/capsule separation attitude and attitude rate uncertainties, and limited knowledge of the flight-day atmospheric properties (density and winds). Additionally, computational uncertainty with the aerodynamic analysis and uncertainties with the parachute deployment algorithm are contributing sources of uncertainty. The mission uncertainties that are considered in the Monte Carlo analysis are grouped into two categories (exoatmospheric and atmospheric) and are listed in Tables 2 and 3, respectively, along with their corresponding 3–σ variances. A Gaussian distribution is utilized for sampling the variation in each parameter.

III. Results and Discussion

A. Nominal MER Entry

To overcome the effects of the high 840 kg entry design mass, the nominal MER entry utilizes a fairly shallow planet-relative flight-path angle of −12 deg as compared with the MPF entry of −13.8 deg. Note, the final entry masses of the two MER Landers are a little lower than this design mass value used in the analysis. This shallow entry was necessary to increase the parachute deployment altitude so that sufficient timeline was available for performing the remaining terminal EDL events (as described in Fig. 1). Consequently, MER will entry with the shallowest flight-path angle of any Mars mission to date. However, this shallow flight-path angle coupled with a lower entry velocity have the advantage of reducing the entry heating and deceleration environments compared with MPF. A peak heat rate value of 50 W/cm^2 and deceleration of 6.4 Earth g is experienced by MER compared with approximately 105 W/cm^2 and 16 Earth g for MPF, respectively.

The nominal MER attitude profile is shown in Fig. 8. Note, α_T is used to denote capsule attitude because the capsule is axisymmetric, where α_T is the included angle between the capsule axis of symmetry and the atmospheric-relative velocity vector. Also illustrated are the various aerodynamic flow regimes during the descent. The MER entry attitude is targeted to 0 deg at atmospheric interface. Before

atmospheric interface, the capsule is in the free molecular flow regime and exhibits a nonzero attitude as a consequence of the inertial pointing from cruise-stage separation. The attitude decreases toward zero as the atmospheric interface point approaches. As the capsule descends into the atmosphere, aerodynamic forces begin to build that cause the capsule to trim to a nonzero α_T.

In the transitional regime, the capsule attitude is observed to increase to $\sim$1 deg. As the capsule continues the descent into the continuum regime, the first of the two static instabilities is encountered as predicted by the aerodynamics, and an abrupt increase in α_T to a little over 2 deg is observed at 125 s. As the capsule passes through this instability, it becomes aerodynamically stable again resulting in a decrease in the attitude down to $\sim$1 deg near the peak heating region of the entry. At approximately 190 s, the capsule encounters the second static instability as seen by another abrupt increase in α_T to almost 3 deg. Upon continued descent, the capsule becomes statically stable again, and the attitude decreases to small values (<0.5 deg) until the start of the supersonic regime. A final increase in attitude is observed below Mach 3 (time of 275 s) as a consequence of the capsule being dynamically unstable at low angles of attack as described by the aerodynamics. The attitude increases to $\sim$1 deg at parachute deployment.

Parachute deployment nominally occurs at 304 s at a target value of 725 N/m^2. A parachute deployment algorithm, which utilizes accelerometer measurements during the descent, initiates the deployment process. This nominal targeted deployment dynamic pressure value is higher than the 600 N/m^2 used by MPF. This value was selected to provide sufficient time for performing all the remaining terminal EDL events as shown in Fig. 1, and may be reduced prior to landing. However, as the parachute deployment dynamic pressure is

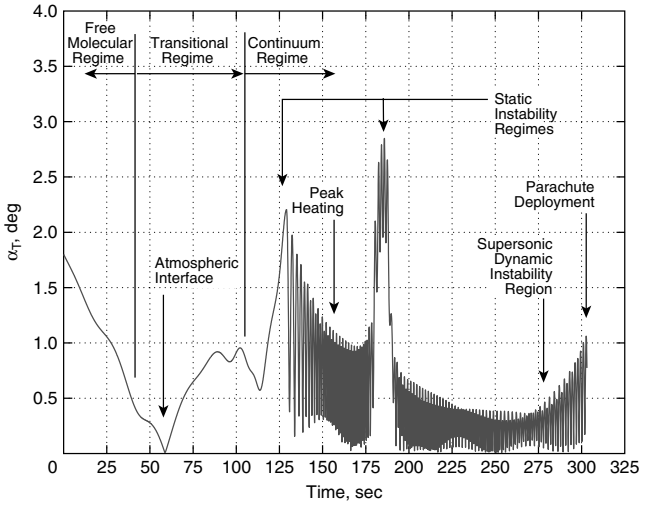

Fig. 8 Nominal capsule entry attitude profile.

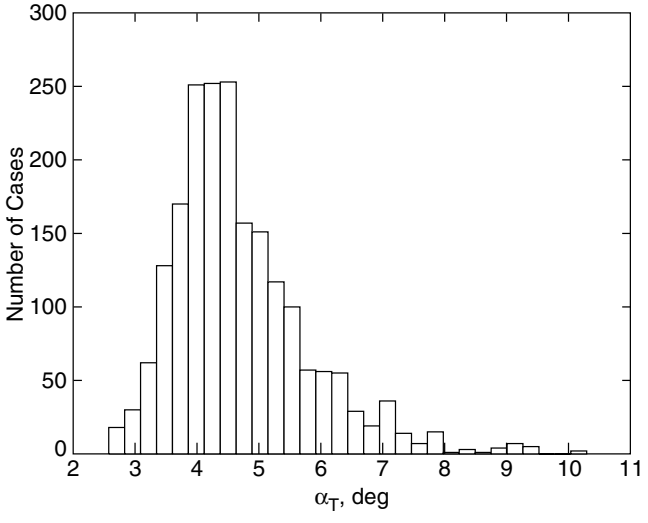

Fig. 9 Distribution of capsule attitude at atmospheric interface.

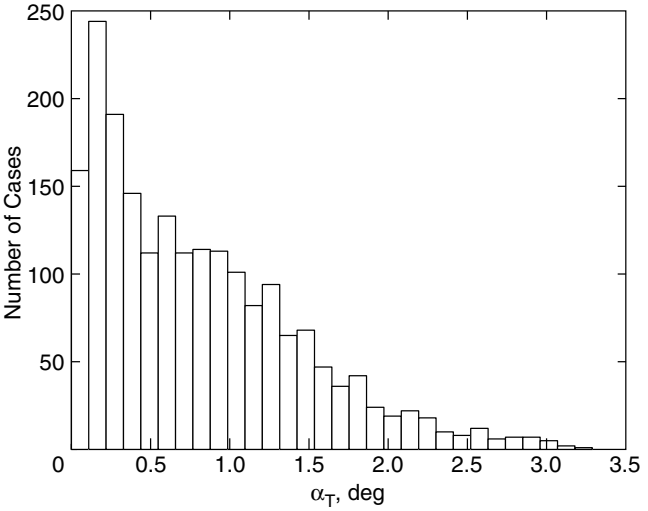

Fig. 10 Distribution of capsule attitude at peak heating.

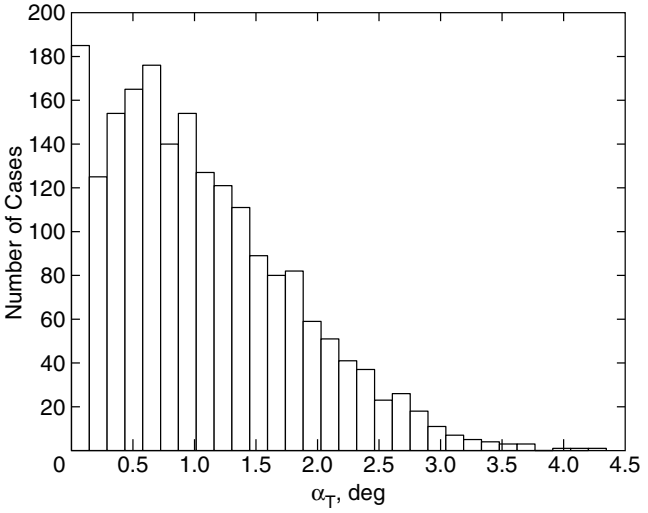

Fig. 11 Distribution of capsule attitude at parachute deployment.

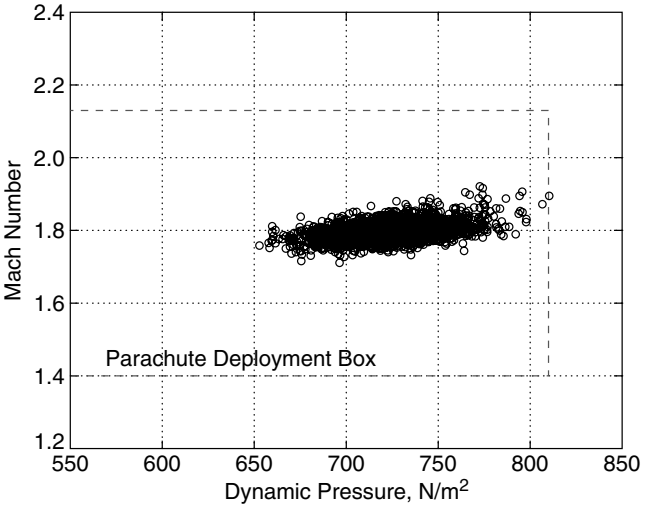

Fig. 12 Variation in parachute deployment conditions.

Table 4 Monte Carlo dispersion analysis statistics.

	Mean	Min	Max	3–σ
Attitude at Atmospheric interface, deg	4.7	2.6	10.3	3.3
Attitude at peak heating, deg	0.8	0.0	3.3	1.9
Attitude at parachute deployment, deg	1.1	0.0	4.4	2.3
Parachute deployment dynamic pressure, N/m^2	723	653	811	71
Parachute deployment Mach number	1.79	1.71	1.92	0.08
Peak heat rate, W/cm^2	42.6	38.6	46.6	3.3
Integrated heat load, J/cm^2	2784	2568	3035	211.3
Peak deceleration, Earth g	6.4	5.8	6.9	0.47

reduced, the capsule attitude will continue to grow beyond that shown in Fig. 8. As a result, a lower bound exists that cannot be exceeded to avoid concerns of large attitudes at deployment that may pose problems for a successful parachute inflation.

B. Monte Carlo Dispersion Analysis

To statistically assess the robustness of the MER entry design, off-nominal conditions are simulated to address uncertainties that may arise during the descent. The impact of multiple uncertainties occurring simultaneously is ascertained by performing a Monte Carlo dispersion analysis. Two thousand random, off-nominal trajectories are simulated varying the parameters listed in Tables 2 and 3 (between their respective upper and lower bounds) to confirm that the MER entry satisfies the design requirements to within 99% (i.e., 99% of the cases should be within the design requirements).

The results from the Monte Carlo dispersion analysis are graphically presented in Figs. 9–12 and tabulated in Table 4. Figures 9–11 show the distribution in the capsule attitude at atmospheric interface, peak heating, and at parachute deployment, respectively. At atmospheric interface, the statistical mean total angle of attack is 4.7 deg, with an observed maximum α_T of 10.1 deg. This variation in α_T at atmospheric interface is entirely a result of the uncertainty in the cruise-stage/capsule separation dynamics. As the capsule encounters the atmosphere, aerodynamic stability damps the attitude to small values so that by peak heating, the mean α_T is 0.8 deg with a maximum of 3.3 deg. As the capsule approaches parachute deployment, the dynamic aerodynamic instability increases the attitude to a mean α_T of 1.1 deg with a maximum of 4.4 deg. These attitudes are well within the design requirement of having 99% of the cases be below 10 deg at atmospheric interface and peak heating, and 13 deg at parachute deployment; only a few outlier cases approach the 10 deg limit at atmospheric interface. The resulting conditions at parachute deployment are shown in Fig. 12, where a scatter plot illustrates the deployment dynamic pressure verses Mach number for each case simulated. The actual design upper limit on the parachute dynamic pressure is over 900 N/m^2. However, to maintain margin, the simulation limit has been set to 810 N/m^2. Because the maximum attitude at parachute deployment only reaches 4.4 deg, there is margin available to reduce the dynamic pressure at deployment (below the minimum value of 653 N/m^2) until the 13 deg attitude limit is reached.

IV. Conclusions

The Mars Exploration Rover (MER) mission successfully landed two rovers that are carrying out scientific investigation of the surface of Mars. Both Landers delivered the rovers to the surface utilizing the same entry, descent, and landing (EDL) scenario that was developed and successfully implemented by the Mars Pathfinder mission. The Landers decelerated with the aid of an aeroshell, a supersonic parachute, retrorockets, and air bags for safely landing on the surface. During the atmospheric flight, the capsules relied solely on aerodynamic stability for traversing all flight regimes to minimize any attitude excursions. To demonstrate that all entry constraints are satisfied, a six-DOF entry trajectory analysis was performed. Through this premission investigation, the capsule aerodynamics and six-DOF entry dynamics were defined.

Aerodynamic analysis of the MER entry has shown that the capsule is aerodynamically stable throughout most of the atmospheric flight. However, at two specific locations during the entry (velocity of 5.5 km/s and 3.6 km/s), the capsule is found to be statically unstable at low angles of attack. Also, at supersonic speeds, the capsule is observed to be dynamically unstable again for low angles of attacks. These instabilities cause abrupt increases in the capsule attitude. However, in all of the flight regimes, the capsule is aerodynamically stable at higher angles of attack. Therefore, any increase in attitude resulting from these instabilities is bounded. A maximum angle of attack of 3 deg is observed for the nominal MER entry.

A Monte Carlo dispersion analysis was performed to statistically assess the premission robustness of the MER entry design to off-nominal conditions that may arise during the descent. The results show that the attitude at peak heating and parachute deployment are well within entry limits of 10 and 13 deg, respectively. A maximum attitude of 3.3 deg at peaking heating and 4.4 deg at parachute deployment is observed. In addition, the variation in the parachute deployment dynamic pressure and Mach number are also well within the design requirements. Reconstruction analysis in under way to assess how well these premission results compare to the actual entries experienced.

Acknowledgements

The authors would like to extend their appreciation to all the members of the MER EDL design team for their contributions. However, specifically, the authors would like to thank Chia-Yen Peng for estimating the cruise-stage/capsule separation dynamics, David Kass for development of the atmosphere model, and Ben Riggs for calculating the capsule mass properties, all of who work at the Jet Propulsion Laboratory.

References

[1] Roncoli, R. B., and Ludwinski, J. M., "Mission Design Overview for the Mars Exploration Rover Mission," AIAA Paper 2002-4823, August 2002.

[2] Spencer, D. A., Blanchard, R. C., Braun, R. D., Kallemeyn, P. H., and Thurman, S. W., "Mars Pathfinder Entry, Descent, and Landing Reconstruction," *Journal of Spacecraft and Rockets*, Vol. 36, No. 3, May–June 1999, pp. 357–366.

[3] Steltzner, A., Desai, P. N., Lee, W. J., and Bruno, R., "The Mars Exploration Rovers Entry Descent and Landing and the Use of Aerodynamic Decelerators," AIAA Paper 2003-2125, May 2003.

[4] Braun, R. D., Powell, R. W., Engelund, W. C., Gnoffo, P. A., Weilmunster, J. K., and Mitcheltree, R. A., "Mars Pathfinder Six-Degree-of-Freedom Entry Analysis," *Journal of Spacecraft and Rockets*, Vol. 32, No. 6, November–December 1995, pp. 993–1000.

[5] Lebeau, G. J., "A Parallel Implementation of Direct Simulation Monte Carlo Method," *Computer Methods in Applied Mechanics and Engineering*, Vol. 174, 1999, pp. 319–337.

[6] Moss, J. N., Wilmoth, R. G., and Price, J. M., "DSMC Simulations of Blunt Body Flows for Mars Entries: Mars Pathfinder and Mars Microprobe Capulses," AIAA Paper 97-2508, 1997.

[7] Cheatwood, F. M., and Gnoffo, P. A., "A User's Manual for the Langley Aerothermodynamic Upwind Relaxation Algorithm (LAURA)," NASA TM-4674, April 1996.

[8] Ingoldby, R. N., Michel, F. C., Flaherty, T. M., Doty, M. G., Preston, B., Villyard, K. W., and Steel, R. D., "Entry Data Analysis for Viking

Landers 1 and 2: Final Report," NASA CR-159388, Nov. 1976.

[9] Gnoffo, P. A., Braun, R. D., Weilmunster, J. K., Mitcheltree, R. A., Engelund, W. C., and Powell, R. W., "Prediction and Validation of Mars Pathfinder Hypersonic Aerodynamic Database," *Journal of Spacecraft and Rockets*, Vol. 36, No. 3, May–June 1999, pp. 367–373.

[10] Schoenenberger, M., Hathaway, W., Yates, L., and Desai, P. N., "Ballistic Range Testing of the Mars Exploration Rover Entry Capsule," AIAA Paper 2005-0055, January 2005.

[11] Steinberg, S., "Experimental Pitch Damping Derivatives for Candidate Viking Entry Configurations at Mach Numbers from 0.6 Through 3.0," Martin Marietta Corporation TR 3709005, Denver Colorado, June 1970.

[12] Schoenenberger, M., Cheatwood, F. M., and Desai, P. N., "Static Aerodynamics of the Mars Exploration Rover Entry Capsule," AIAA Paper 2005-0056, January 2005.

[13] Brauer, G. L., Cornick, D. E., and Stevenson, R., "Capabilities and Applications of the Program to Optimize Simulated Trajectories (POST)," NASA CR-2770, Feb. 1977.

[14] Desai, P. N., and Cheatwood, F. M., "Entry Dispersion Analysis for the Stardust Comet Sample Return Capsule," *Journal of Spacecraft and Rockets*, Vol. 36, No. 3, May–June 1999, pp. 463–469.

[15] Desai, P. N., and Cheatwood, F. M., "Entry Dispersion Analysis for the Genesis Sample Return Capsule," *Journal of Spacecraft and Rockets*, Vol. 38, No. 3, May–June 2001, pp. 345–350.

D. Spencer
Associate Editor